Scanning Microscopy

Volume 1993
Number 7 *Physics of Generation and Detection of Signals Used for Microcharacterization*

Article 4

1993

Efficiency of the Secondary Electron Detector in the Scanning Electron Microscope

Zbigniew Czyzewski
University of Tennessee, Knoxville

David C. Joy
University of Tennessee, Knoxville

Scanning Microscopy Supplement 7, 1993 (Pages 33-38) 0892-953X/93$5.00+.25
Scanning Microscopy International, Chicago (AMF O'Hare), IL 60666 USA

EFFICIENCY OF THE SECONDARY ELECTRON DETECTOR IN THE SCANNING ELECTRON MICROSCOPE

Zbigniew Czyzewski* and David C. Joy[1]

Electron Microscope Facility, F239 WLSB, University of Tennessee, Knoxville, TN 37831
[1]Also Oak Ridge National Laboratory, Oak Ridge, TN 37831

Abstract

The efficiency of the secondary electron detector in the scanning electron microscope (SEM) is one of the most important factors affecting the imaging process of the SEM. To compute the detector efficiency, the electrostatic field inside a specimen chamber must be known. A simple way of performing such calculations is to use a spreadsheet program which has a built-in capability of storing and performing some operations on three-dimensional matrices. Using a spreadsheet program makes it possible to solve the Laplace equation and calculate electron trajectories in geometrically complex electrostatic fields. This technique is applied to the estimation of detector efficiency in the SEM.

Key Words: Detector efficiency, scanning electron microscope, electrostatic field, Laplace equation, electron trajectory, Monte Carlo simulation.

*Address for correspondence and present address:
Zbigniew Czyzewski,
CSI,
835 Innovation Dr.,
Knoxville, TN 37932, USA
Phone No.: (615) 675 2400
FAX No.: (615) 675 3100

Introduction

The electron microscope uses an electron beam to obtain various kinds of information about specimens. The electron beam is focussed by electrostatic and magnetic fields, and electron detectors employ electrostatic fields to attract or deflect electrons. In many cases, the demand to calculate the electron trajectories in a fast and visual way is very strong. Unfortunately, Monte Carlo calculations of secondary electron emission rarely take into consideration the efficiency of an electron detector even when theoretical data have been compared with experimental ones. Recently, however, Suga *et al.* (1990) incorporated the detector field into their calculations to estimate the SEM images quantitatively.

When the total secondary electron emission yield is studied, a special semi-circular detector can be used and detector efficiency does not have to be considered. However, for other detector types, especially the Everhart-Thornley (ET) detector, used in the SEM it is sometimes necessary to include the detector efficiency when comparing with experimental data. The most critical problem is simulating the secondary electron signal for the ET detector from specimen shapes other than planar. Most of the proposed topographical reconstruction methods do not consider the detector efficiency at all, mainly because they are based on a two signal ratio approach and because the detector efficiency is different for various ET detectors provided by different vendors. Scanning microscope vendors try to optimize the ET detector efficiency and estimate it for various working conditions using sophisticated software. However, recently many researchers have been using spreadsheets to calculate the electrostatic potential (Leclerc and Sanche, 1990; Orvis, 1987; Czyzewski and Joy, 1992), and it is possible to write a spreadsheet application to determine an electron trajectory inside any chamber and even estimate the detector efficiency for a given chamber geometry and a parameter set.

In this paper, an application of a spreadsheet program (Lotus 1-2-3, release 3.1+) to compute the electron trajectories in a truly three-dimensional space is presented. A similar application but two-dimensional

was described by Bradley and Joy (1991). The Laplace equation can be solved in a simple and visual way. The advantage of the spreadsheet for this problem lies in the ease of performing each step: initialization of the boundary conditions, iterative solution of the Laplace equation and calculation of trajectories.

The Laplace Equation

The Laplace equation is solved by an explicit finite-difference method, which is based on the discretization of space and the central difference approximation for the derivative. In a three-dimensional space composed of cubic cells of dimension Δ^3, the Laplace equation takes the form:

$$\phi(i, j, k) = [\phi(i+1, j, k) + \phi(i-1, j, k) + \phi(i, j+1, k) + \phi(i, j-1, k) + \phi(i, j, k+1) + \phi(i, j, k-1)]/6, \quad (1)$$

where $(i, j, k) = (x_n/\Delta, y_n/\Delta, z_n/\Delta)$ is the coordinate, in Δ units, of the grid point characterizing cell n.

The potential at a point (i,j,k) is therefore simply the average of the potentials in the immediate surrounding points, a property of several scalar fields. As calculations are performed, the boundaries will send their potential to their neighborhood, expand and mix through space until a convergence is attained (that is, the potential at any point does not change significantly with further calculations). The information given by the boundaries has therefore traveled through space, and the scalar field is completely defined from explicit dependence stated by equation (1). Using a spreadsheet to perform potential calculations is very easy and, most importantly, is a visual process. In the three-dimensional spreadsheet space one has to draw the boundary of the chamber and apply the bias values to it. This process can be relatively slow for very complicated geometries. Finally, the other inner cells of the volume of interest are assigned the average function for adjacent cells to model equation (1). A short macro starts the calculation, and one may observe the convergence of the potential in any region of the spreadsheet.

To illustrate this approach, the geometry of the Hitachi S-800 chamber was copied in a coarse approximation into a spreadsheet as a 21 by 53 by 53 matrix. The chamber height was assumed to be 20 mm and the diameter 52 mm; the detector diameter was assumed to be 8 mm and its length inside the chamber 1 mm. Figure 1 shows results for the electrostatic field in the form of equipotential lines for a grounded specimen and a +200 V detector bias. The field around the specimen is very weak.

Electron Trajectories

Once the potentials are calculated, it is easy to compute the electron trajectories within the same spreadsheet file. Trajectory calculations visualize the origin of the divergence between potential settings suggested by standard electron optics and those necessary to achieve maximum current in the real system. From the many approaches to trajectory calculation, the parametric solution of Newton's second law with respect to time and adimensional spatial units was chosen. This approach was proposed by Leclerc and Sanche (1990) in their spreadsheet calculations. The three components of the force acting on the electron at a particle position expressed in the Δ units $(x/\Delta, y/\Delta, z/\Delta)$ are calculated from linear approximation of the potential within the grid points surrounding the $(x/\Delta, y/\Delta, z/\Delta)$ trajectory point. Then the spreadsheet calculates the time steps corresponding to an adimensional spatial displacement s in all x, y, and z directions, and the smaller time interval is chosen to compute the subsequent position. The procedure is repeated until a boundary is reached. For s = 1, the electron trajectory is exactly related to the grid resolution, although the smaller s is the smoother is

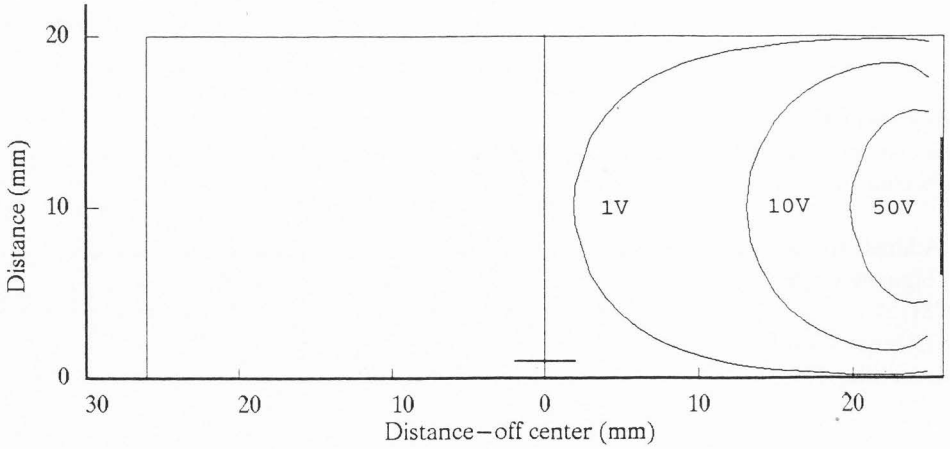

Figure 1. Equipotential lines for the Hitachi S-800 chamber (52 mm x 20 mm); detector bias +200 V; detector located on the right wall of the chamber; sample position - center of the short horizontal bar near the zero of the horizontal scale.

the computed trajectory, and the better the trajectory accuracy is. However, for very small values of displacement, s, the time necessary for trajectory calculation is much longer, while trajectory accuracy is not significantly improved because it is limited by the space interval, Δ, of the potential field. Space charge effects on the trajectories are not taken into account by these calculations, but, for lens systems aberrations, can be monitored graphically. A magnetic field can also be easily incorporated into an electron trajectory calculation, no matter if it is homogeneous or not.

Once the potential field has been calculated, its values might be extracted, if there is memory limitation, and electron trajectories can be computed. Figure 2 shows electron trajectories for the Hitachi S-800 chamber. Because the field around the specimen is very weak, the detector can only attract electrons from its side. The higher the electron energy, the lower the detector efficiency is. Figure 3 presents trajectories for a specimen biased at -100 V. In this case, a very small number of electrons reaches the detector. Electrons are repelled by the specimen field, and, because their energy is at least 100 eV, the detector field cannot attract these electrons unless their trajectories pass close to the detector. A set of trajectories presented in Figures 1 and 2 were chosen, for illustrative purposes, to lie on a plane determined by the center of the detector and the chamber-axis although all calculations were three-dimensional.

Efficiency of the Everhart-Thornley Detector

The efficiency of a conventional secondary detector in the SEM can be defined as a ratio of the number of

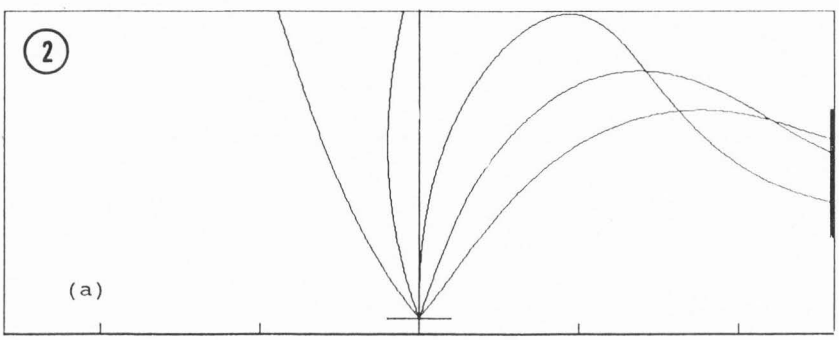

Figure 2. Electron trajectories inside the S-800 chamber; detector and sample position as in Figure 1, in (b) and (c) half of the chamber shown; detector bias +200 V. Electron energy: (**a**) 1 eV, (**b**) 4 eV, (**c**) 10 eV; take-off angles: (**a**) -40°, -20°, 0°, 20°, 40°; (**b**) & (**c**) 0°, 20°, 40°, 60°, 80°.

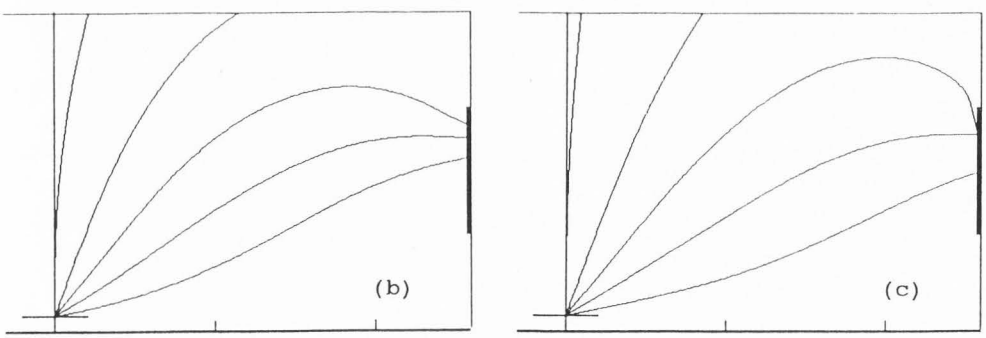

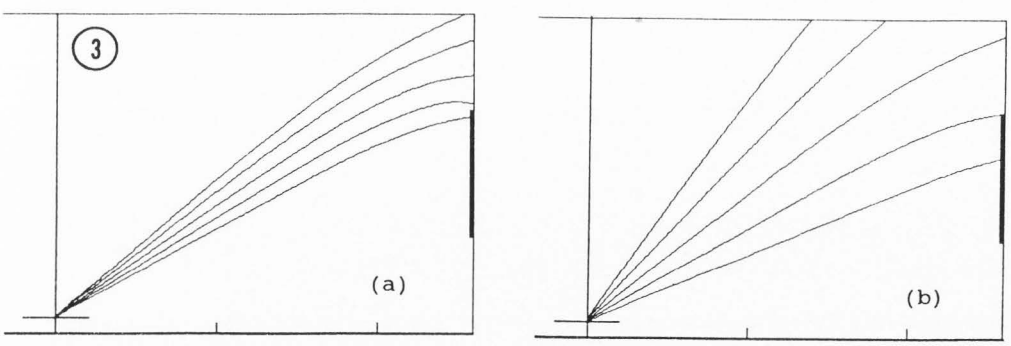

Figure 3. Electron trajectories inside the S-800 chamber; half of the chamber shown; detector and sample position as in Figure 1; detector bias +200 V. Specimen -100 V; take-off angles 0°, 20°, 40°, 60°, 80°; electron energy: (**a**) 1 eV, (**b**) 10 eV.

electrons collected by a detector to the total number of emitted electrons. To determine the detector efficiency, a large number of secondary electron trajectories over the whole range of emission angles has to be calculated. In general, the detector efficiency is a function of the chamber geometry and the detector bias. To study the effects of these two factors, two more chamber geometries were considered. They are depicted in Figure 4. Figure 4a presents the chamber geometry from Figure 1. The geometry in Figure 4b is primarily the same as that in Figure 4a, but the bottom of the chamber is lowered by 5 mm, and therefore this geometry is a better approximation to the real chamber of Hitachi S-800. In the following discussion, the geometry depicted in Figure 4a is named "shallow", and the geometry in Figure 4b "deep". Figure 4c shows a modification of the "deep" geometry with longer detector tube and is named a "long detector" geometry. Although it is possible to estimate a rank of the detector efficiency for these three geometries using other methods, the approach presented above offers not only the raw data on the detector efficiency but also the detailed information about potential field inside the chamber, which makes this approach very helpful in the detection optimization.

Figure 5 presents the detector efficiency as a function of electron energy and detector bias for the "deep" geometry. This figure confirms a well known fact that, when decreasing the electron energy or increasing the detector bias, detector efficiency increases. It was assumed that the angular distribution of secondary electrons is, according to Lambert's law, $\cos\beta$, where β is the take-off angle with respect to the chamber-axis.

The detector efficiency reflects the distribution of the potential field. Therefore, a small increase of the potential on the way from the specimen to the detector for the "deep" geometry in comparison with "shallow" geometry leads to a little increase of the number of electrons reaching the detector (Figure 6). However,

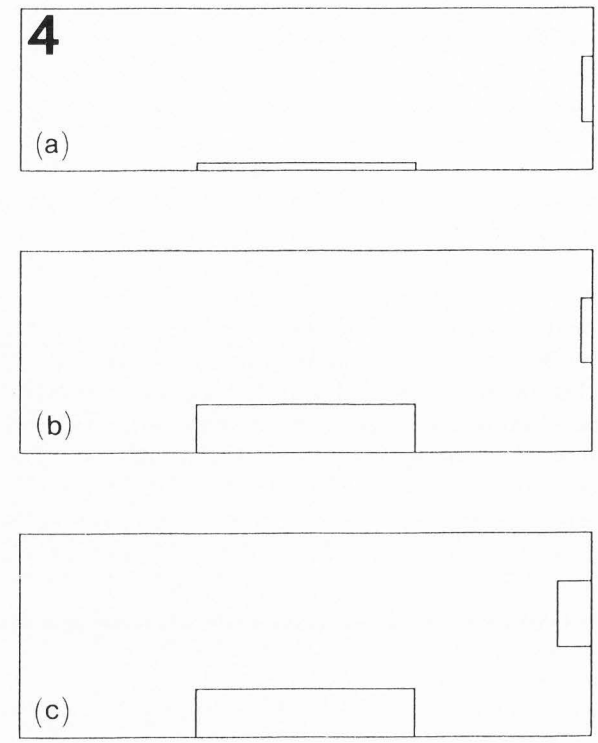

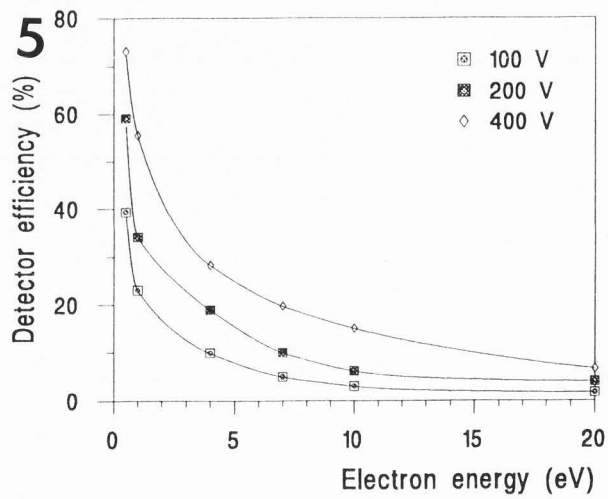

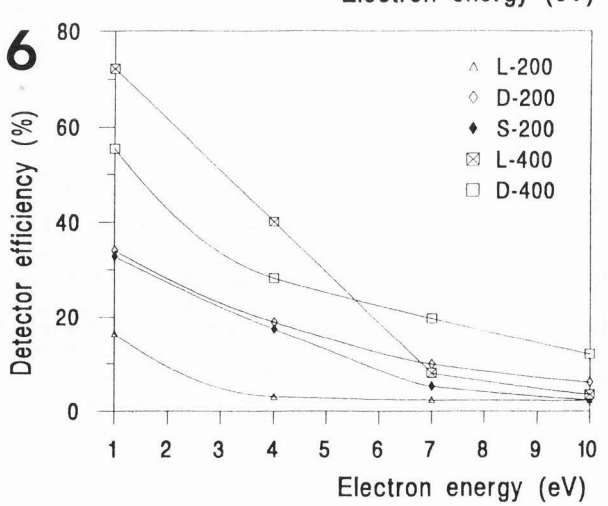

Figure 4 (top). Different geometry approximations to the Hitachi S-800 chamber: (**a**) shallow, as in Figure 1, 52 mm x 20 mm, detector length inside chamber 1 mm; (**b**) deep, 52 mm x 26 mm, (**c**) long detector, 52 mm x 26 mm, detector length 3 mm; detector at the right wall of the chamber, specimen stage in the center at the bottom of the chamber.

Figure 5 (middle). Detector efficiency for chamber geometry shown in Figure 4b as a function of electron energy and detector bias as a parameter.

Figure 6 (bottom). Detector efficiency for chamber geometries shown in Figure 4; L long detector, D deep, and S shallow geometry; 200 and 400 are detector bias values in volts.

the same argument is not sufficient to explain the difference in detector efficiency between the "deep" and "long detector" geometry for a low detector bias. In fact, more electrons are directed towards a detector plane for the "long detector" geometry but the detector efficiency is smaller than in the case of the "deep" geometry for detector bias less than 280 V and for electron energy greater than 0.5 eV. The focusing strength of a detector is much less for "long detector" geometry. This focusing lens is formed by detector and surrounding chamber walls. Such a conclusion can be easily drawn when trajectories and potential fields are calculated in a visual way.

With Monte Carlo simulation of secondary electron generation, the calculation for a single trajectory finishes when the trajectory emerges out of the specimen and there is not any shadowing effect for this trajectory. However, knowing the take-off angle of a trajectory and an acceptance range of the detector, one can determine if an electron will be collected or not. The collection range of a detector can be easily computed using the approach to trajectory calculation presented above.

Discussion

The application of a spreadsheet program to calculation of the electron trajectories in an SEM chamber was presented. The three-dimensional chamber can be modelled and the potential field can be easily calculated in a visual way without having to rely on massive computer facilities. This approach can be successfully used for any type of detector and any electron signal in the SEM as weil as for other charged-particle trajectory calculations.

Acknowledgment

The authors are grateful to AMRAY Inc. for partial support of this work.

References

Bradley GF, Joy DC (1991) Spreadsheet program for calculating secondary electron trajectories in electrostatic fields. Proc. 49th EMSA Meeting. San Francisco Press, 534-535.

Czyzewski Z, Joy DC (1992) Electron trajectories in electrostatic fields. Proc. 50th EMSA Meeting. San Francisco Press, 954-955.

Leclerc G, Sanche G (1990) Spreadsheets for computing charged-particle trajectories in 3-D electrostatic fields. Computers in Physics **Nov 1990**, 617-626.

Orvis WJ (1987) 1-2-3 for Scientists and Engineers. SYBEX, Alameda, California, 1-341.

Suga H, Fujiwara T, Kanai N, Kotera M (1990) Secondary electron image contrast in the scanning electron microscope. Proc. 12th Intern Congress for Electron Microscopy. San Francisco Press, 410-411.

Discussion with Reviewers

F. Hasselbach: What is a spreadsheet program, and what are its advantages compared to conventional ray tracing programs (e.g., the well known Simion program)?

Authors: A spreadsheet program is a program which handles many different operations on matrices. It is usually equipped with high quality graphical user interface. Spreadsheets also provide simple programming language. When using numbers as elements of matrices, a spreadsheet program with its many built-in functions is a very useful tool for different kinds of calculations which require data to be stored in arrays. The advantages of a spreadsheet application over conventional tracing programs are: (**a**) simple and fast preparation of input data (chamber geometry, electrodes' polarization, etc.); (**b**) portability, the program can run on almost every personal computer; (**c**) high quality graphical user interface, the user may watch the dynamics of the calculation process, final data can be presented in many graphical ways; and (**d**) ease of use.

K. Murata: Could you comment the on effect of the magnetic field leaked from the objective lens on electron trajectories or the detector efficiency?

Authors: If the field is small and almost uniform, then the effect is negligible as all of the trajectories will just rotate about the optic-axis somewhat. If the field is very high, then clearly a full simulation of the effects of both E and B would have to be done. This is something that we cannot yet handle but it could be done.

K. Murata: Have you calculated trajectories of electrons ejected from the chamber wall? Have you studied whether the detector efficiency varies with the detector position in the vertical direction?

Authors: We have studied neither of these interesting problems using our spreadsheet application.

M.A. Smith: What is the condition on s? Is s the displacement? If so, is not the smallest discrete value of s Δ?

Authors: The electron trajectory is computed indiscrete points in space using the Newton equation. The distance between two consecutive points is determined, in our application, from the condition that the maximum distance for either direction (X, Y, Z) is equal to s.

Therefore, s is a displacement and, here, is expressed in Δ units. The smallest value of s is 0.

K. Murata: Could you show the exit angle region of electrons to be detected in a polar diagram?
Authors: The exit angle region of electrons is a rapidly varying function of an electron energy and a take-off angle as well as a chamber geometry. For any set of values of these parameters, the exit angle range of electrons to be detected is a binary function of an azimuthal angle. An electron reaches a detector or it does not. This function can be easily obtained in our spreadsheet application. You probably mean the averaged exit angle region over the azimuthal angle range. We have not done such a calculation.

F. Hasselbach: Can you give some data on calculation times and hardware requirements?
M.A. Smith: What kind of computer did the authors use? How long did it take to do calculation for Figure 1? How much computing time and RAM are required for a typical calculation? Can one watch the convergence in three dimensions with the spreadsheet program?
Authors: We used IBM PC 386 with math co-processor and 16 meg RAM. There are minimal hardware requirements for real three-dimensional calculations. The potential calculations are relatively slow, and it took approximately 1 hour to obtain data for Figure 1. One can watch the convergence in three dimensions with the spreadsheet program. Trajectories are calculated relatively fast with an average time of 10 sec for one trajectory.